Blackbody spectra with different temperatures

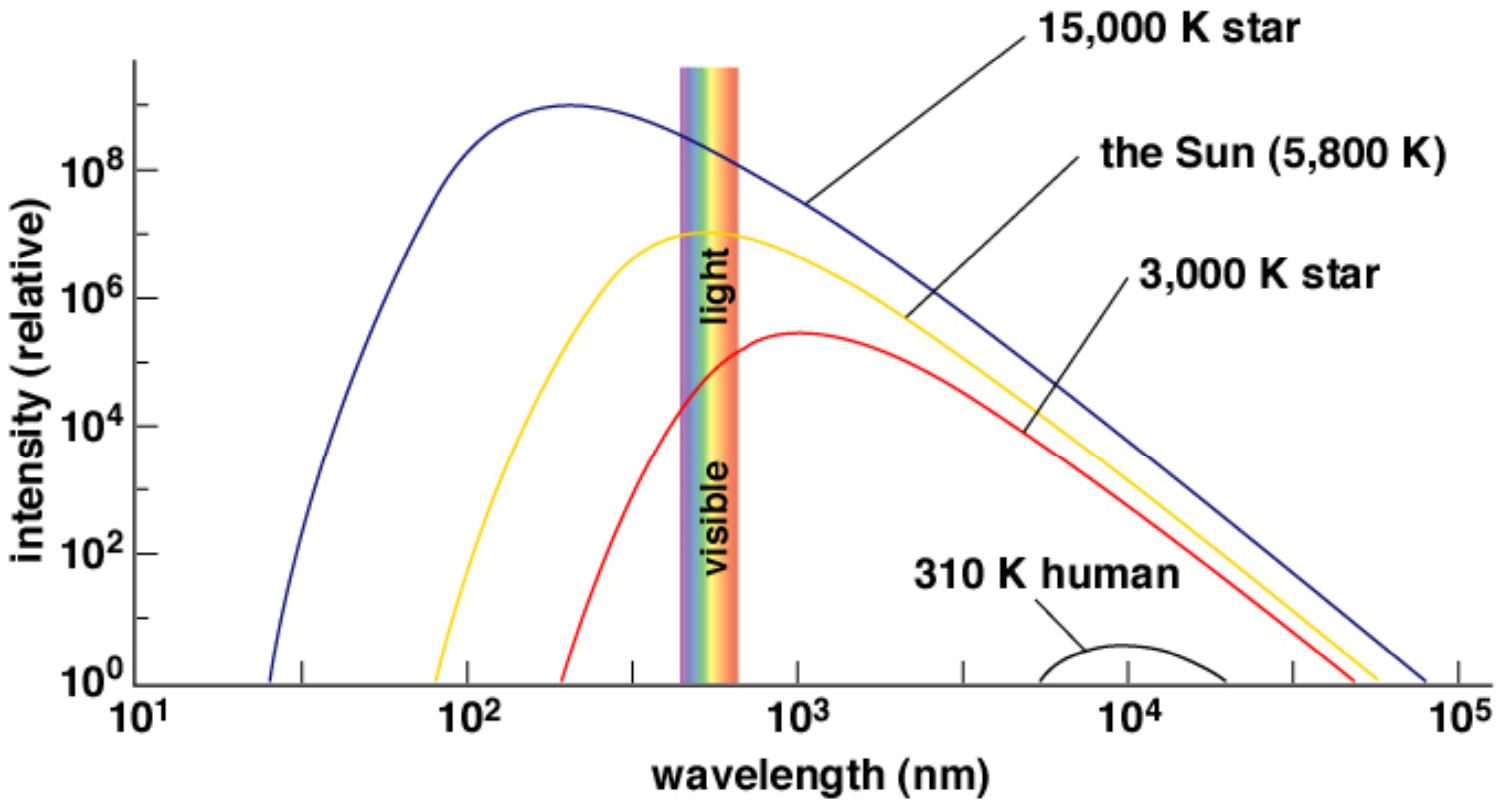

$$B_\nu(T,\nu) = \frac{2h\nu^3}{c^2}\frac{1}{e^{h\nu/kT}-1} \approx \frac{2k\nu^2}{c^2}T$$

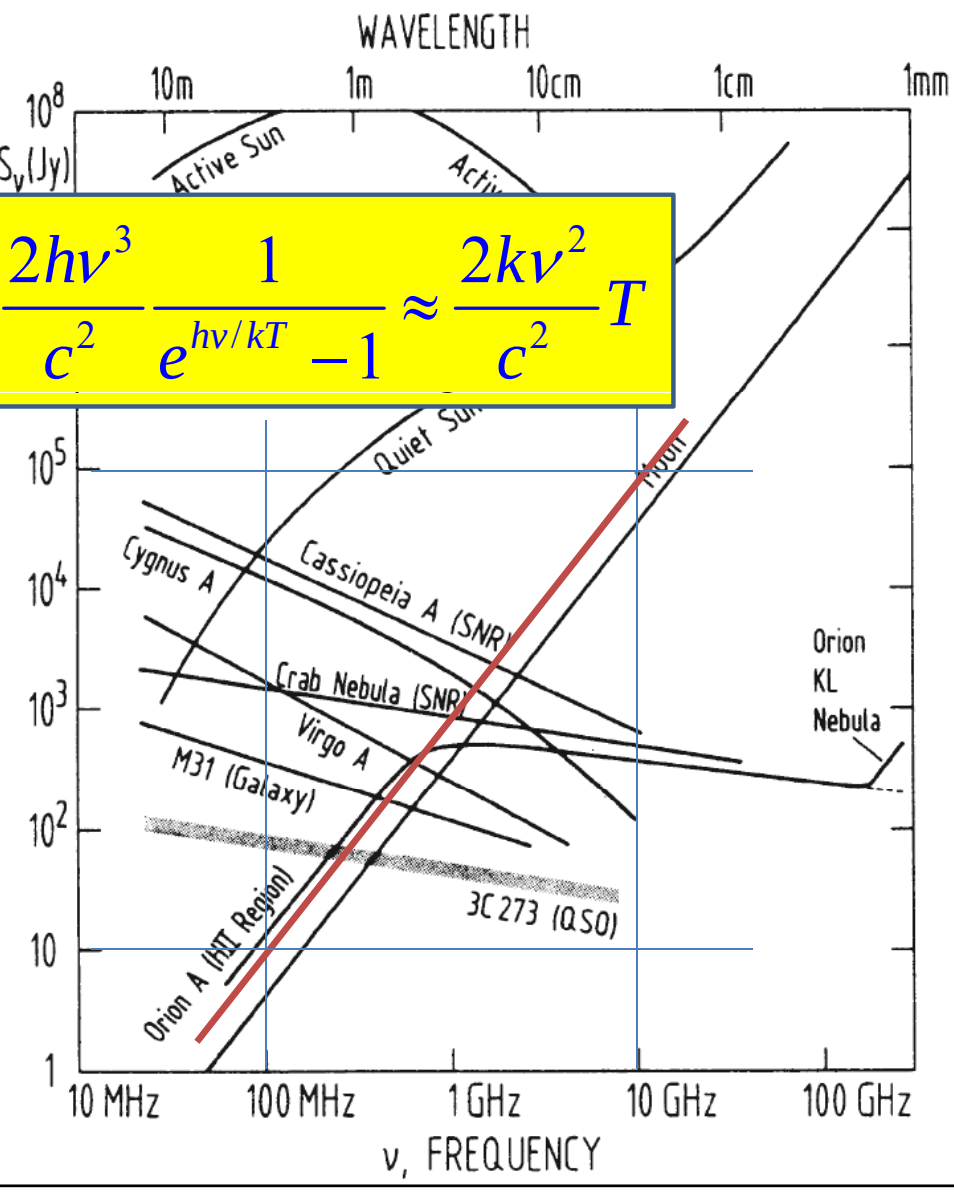

From Rholfs and Wilson (2001)

Radio image of the Galaxy at 408 MHz

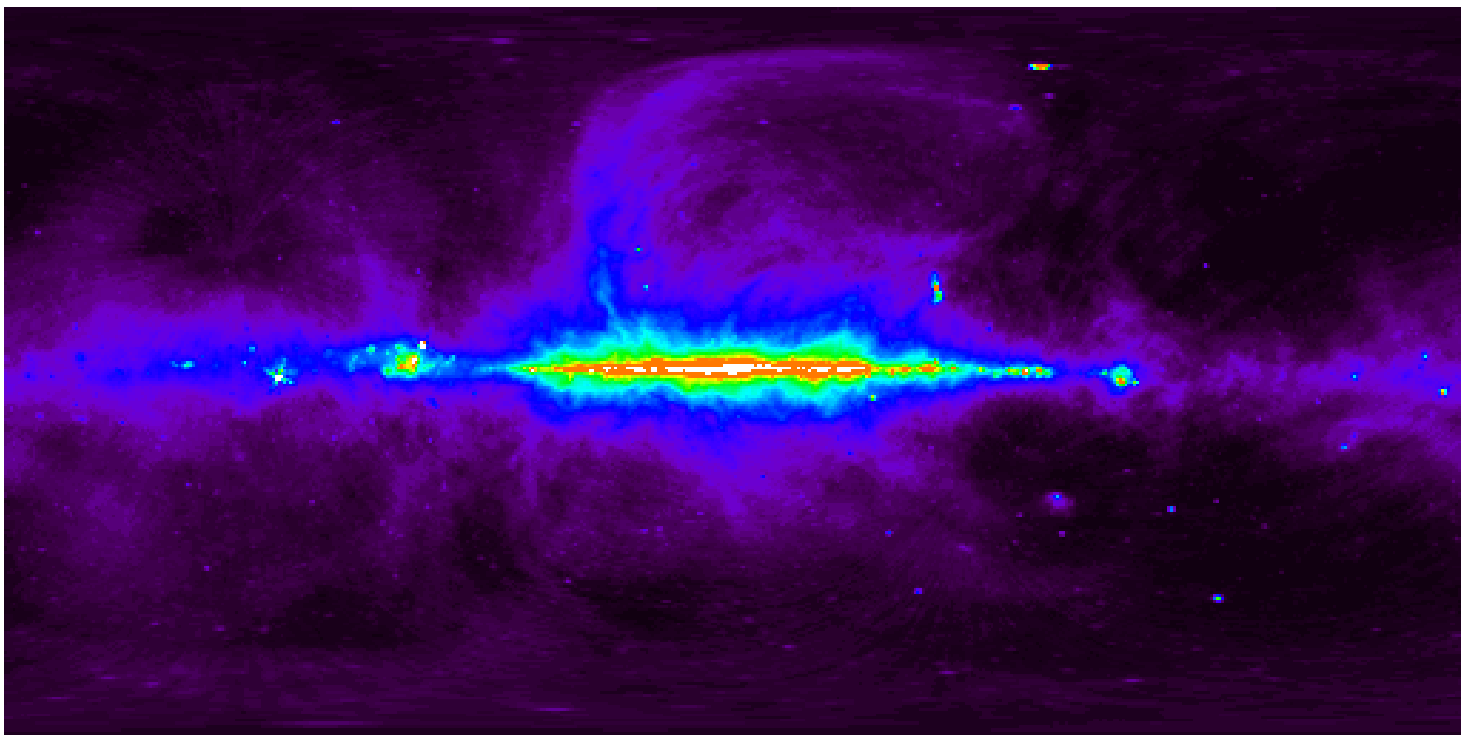

What do we see? Electrons moving close to the speed of light.

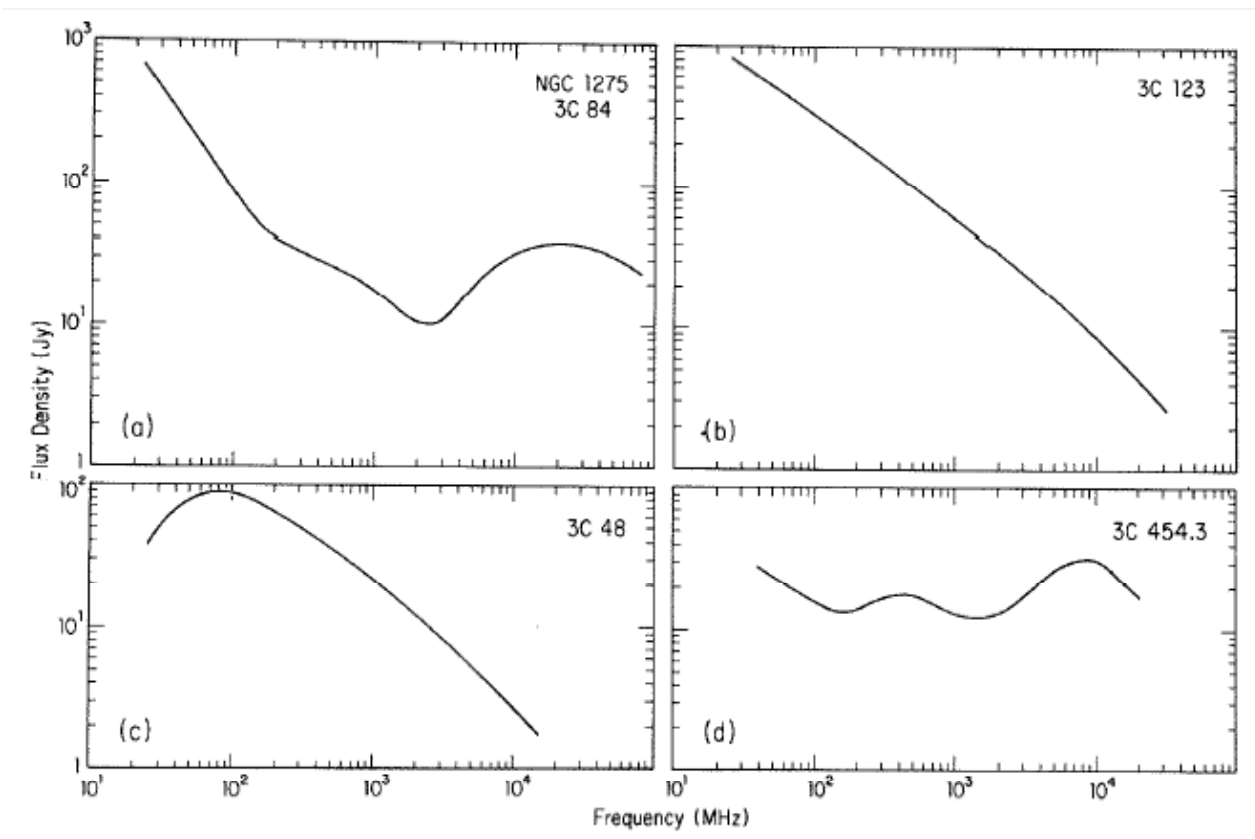

Figure 5.8: Representative spectra of radio galaxies and quasars [111]. The radio source 3C 84 in the nearby galaxy NGC 1275 contains a very compact nuclear component that is opaque below about 20 GHz. The radio galaxy 3C 123 is transparent at all plotted frequencies, and energy losses steepen its spectrum above a few GHz. The quasar 3C 48 is synchrotron self-absorbed only below 100 MHz, while the quasar 3C 454.3 contains structures of different sizes that become opaque at different frequencies.

Blackbody spectra with different temperatures

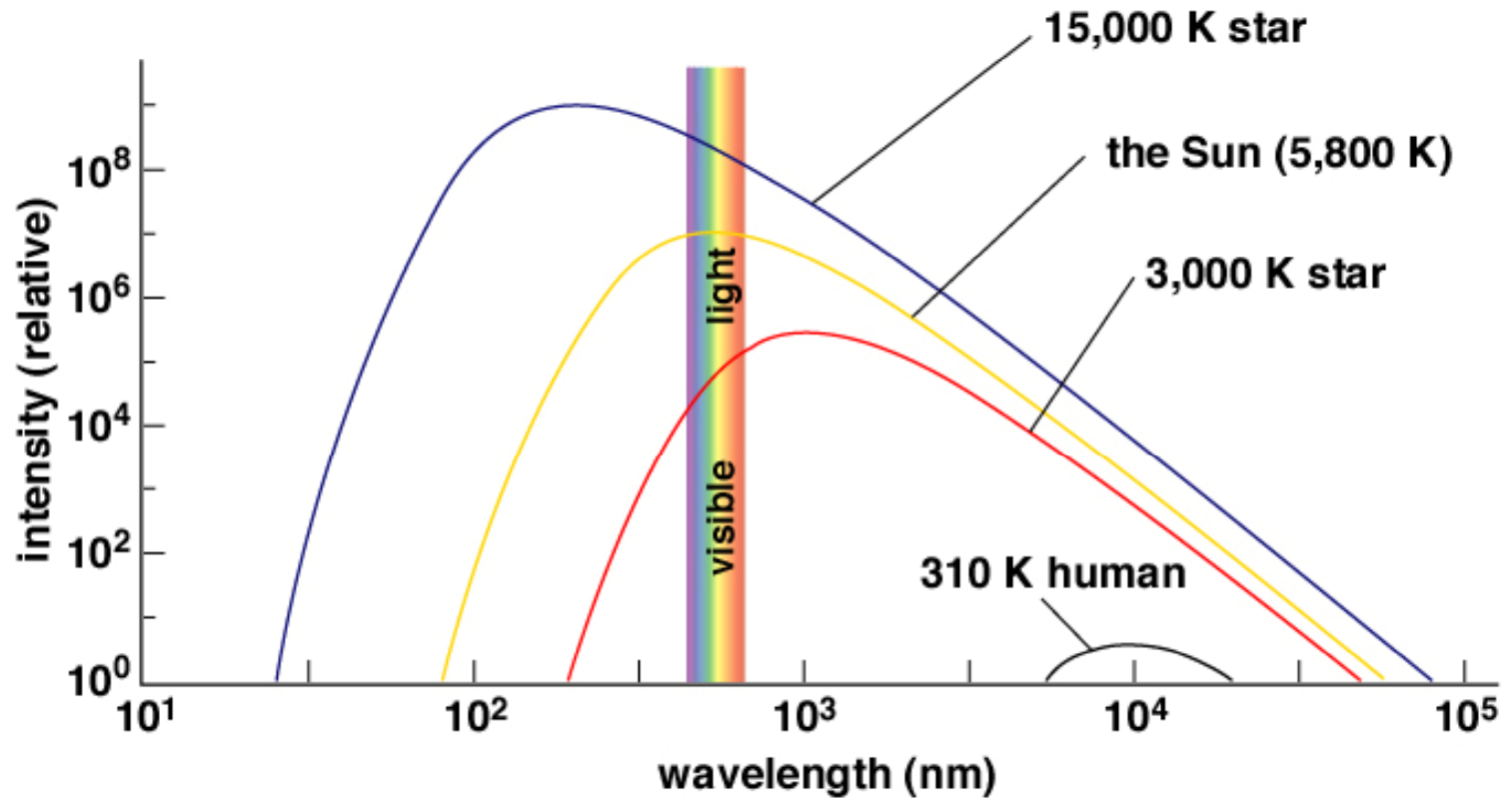

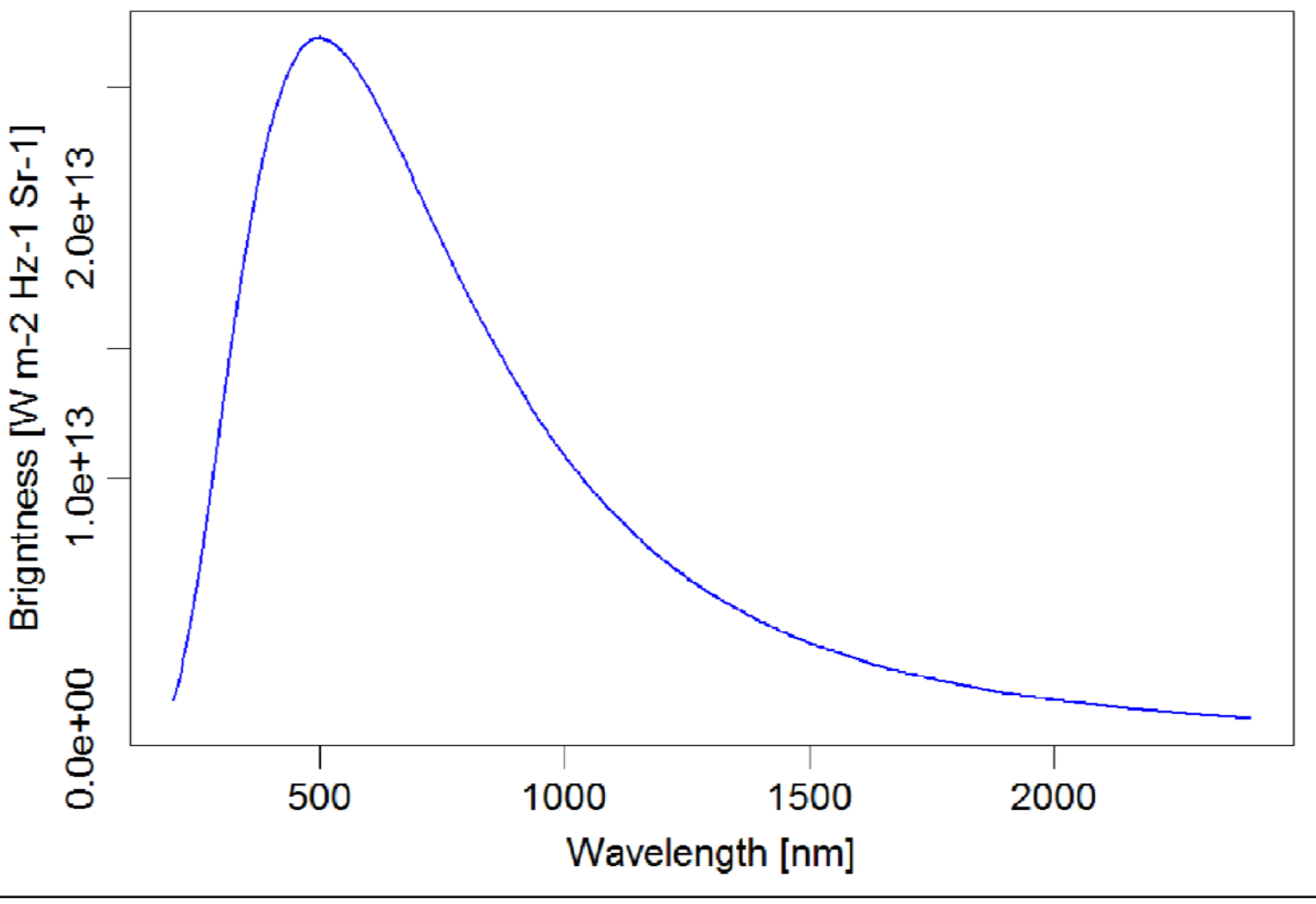

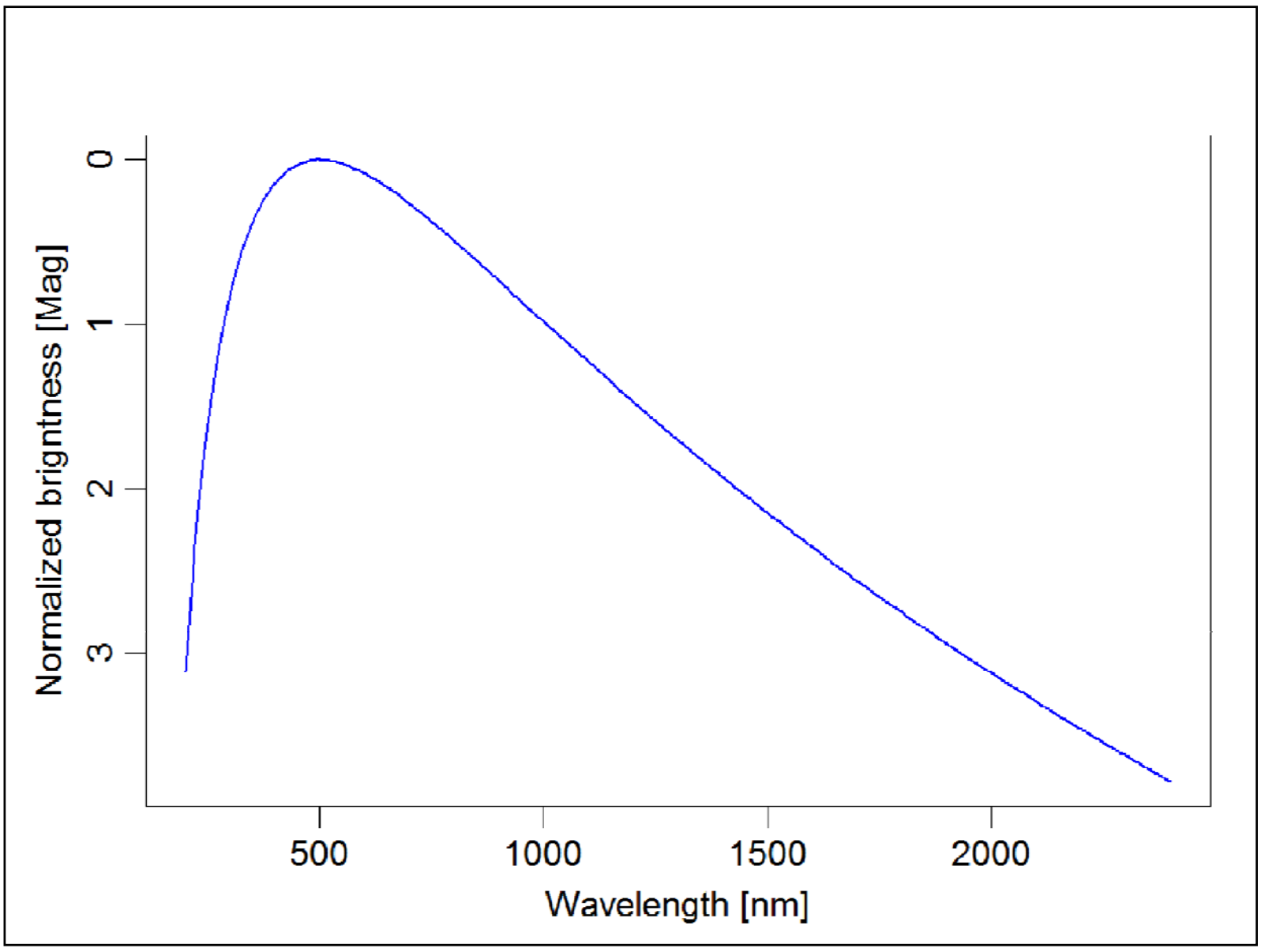
Normalized brigntness [Mag]
0
1
2
3
500
1000
1500
2000
Wavelength [nm]

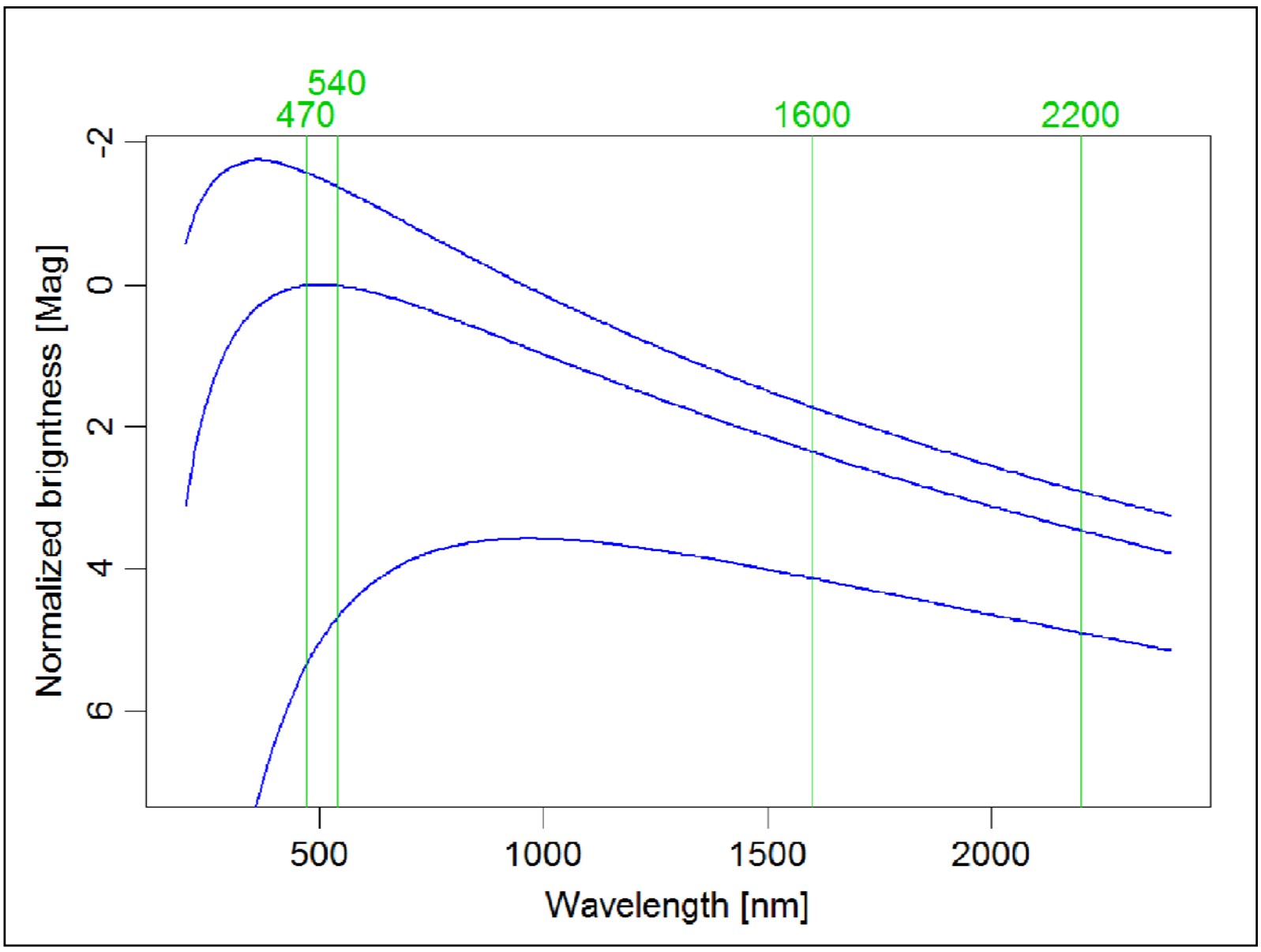
540
470
1600
2200
Normalized brigntness [Mag]
-2
0
2
4
6
500
1000
1500
2000
Wavelength [nm]

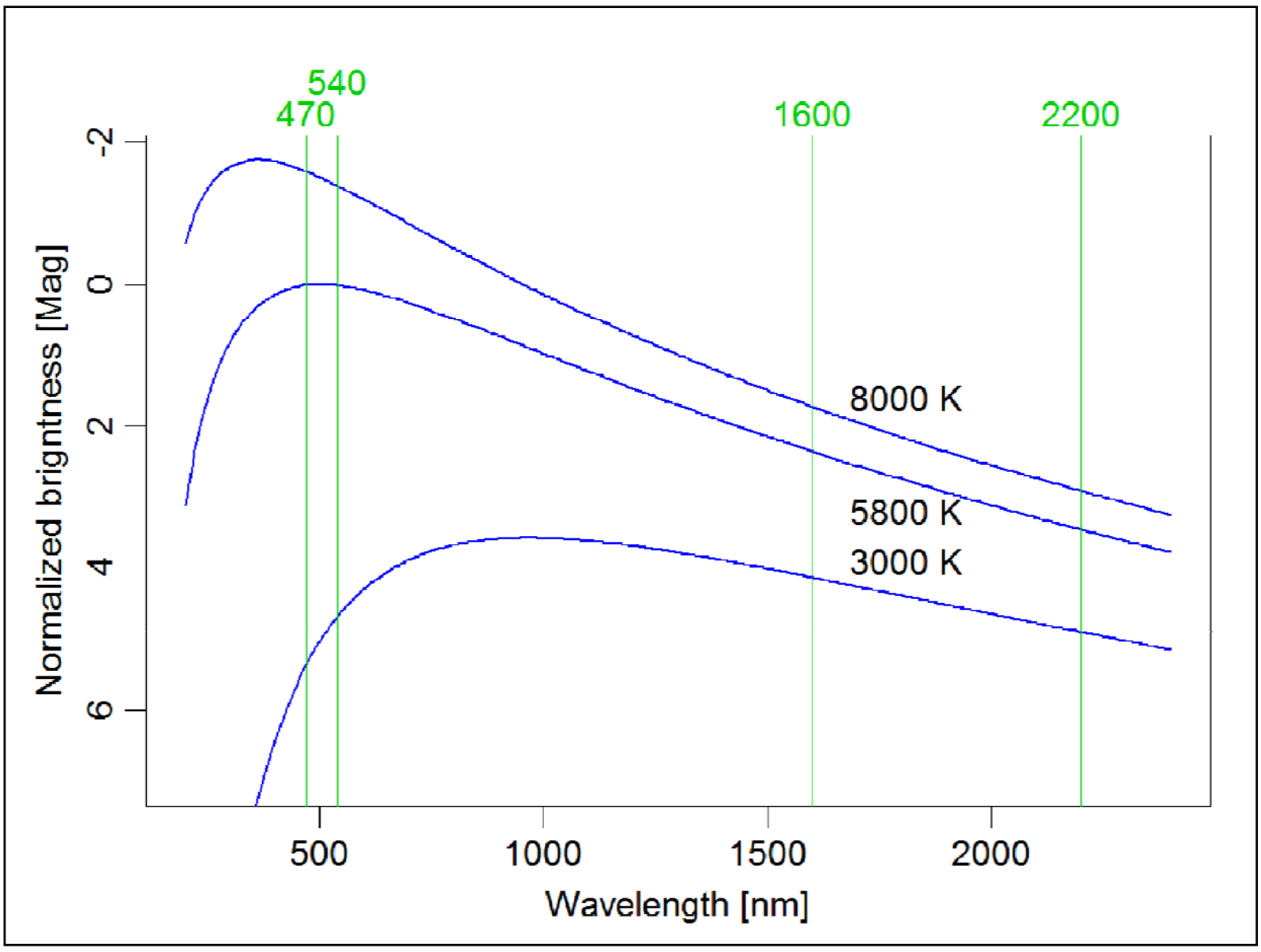

Normalized response for the UBVRI system

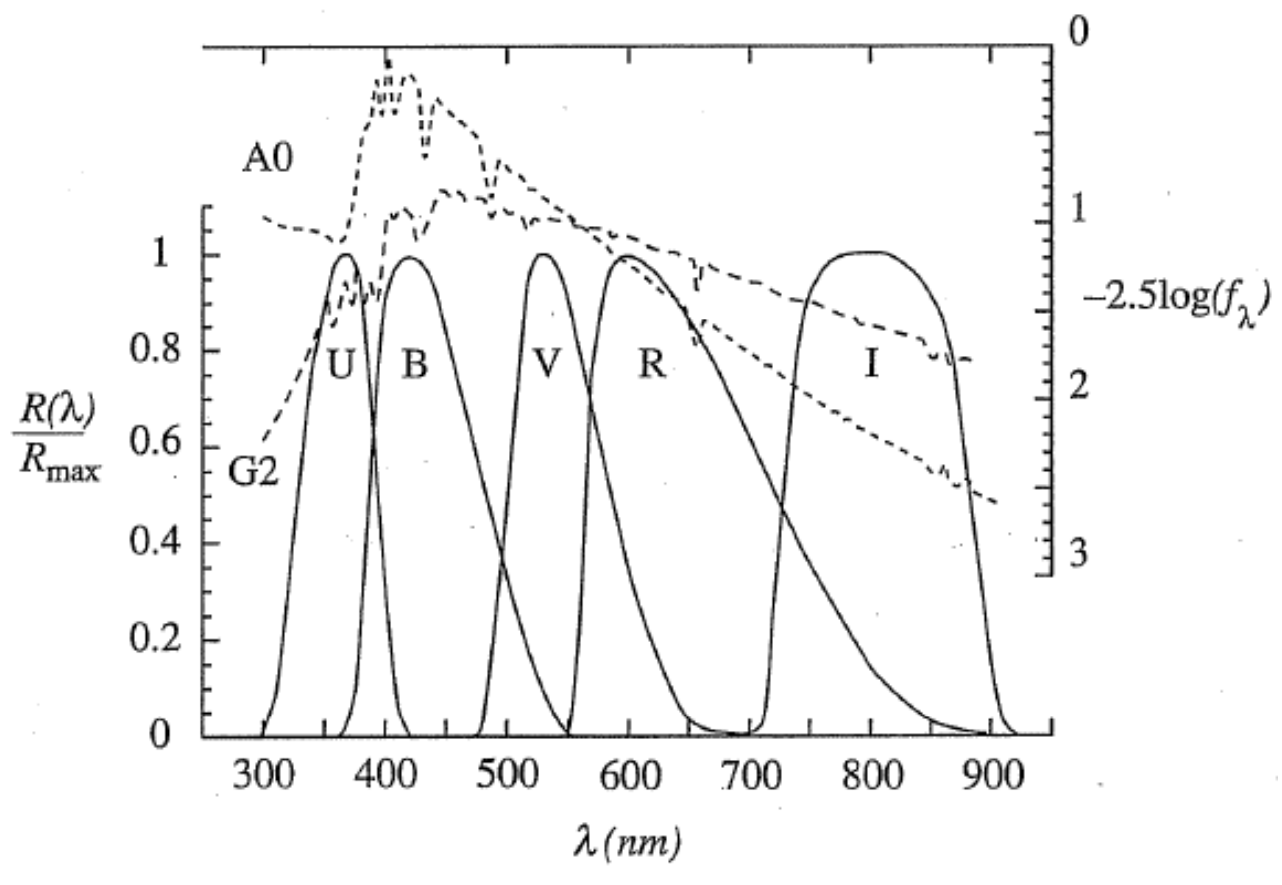

Filter width, effective wavelength

Fig. 10.4 Definitions of the middle and width of a band. The curve shows the function $R(\lambda)$. The mean wavelength divides the area under the curve into two equal parts (shaded and unshaded). The dark-gray rectangle has a width equal to the bandwidth and an area equal to the area under the curve.

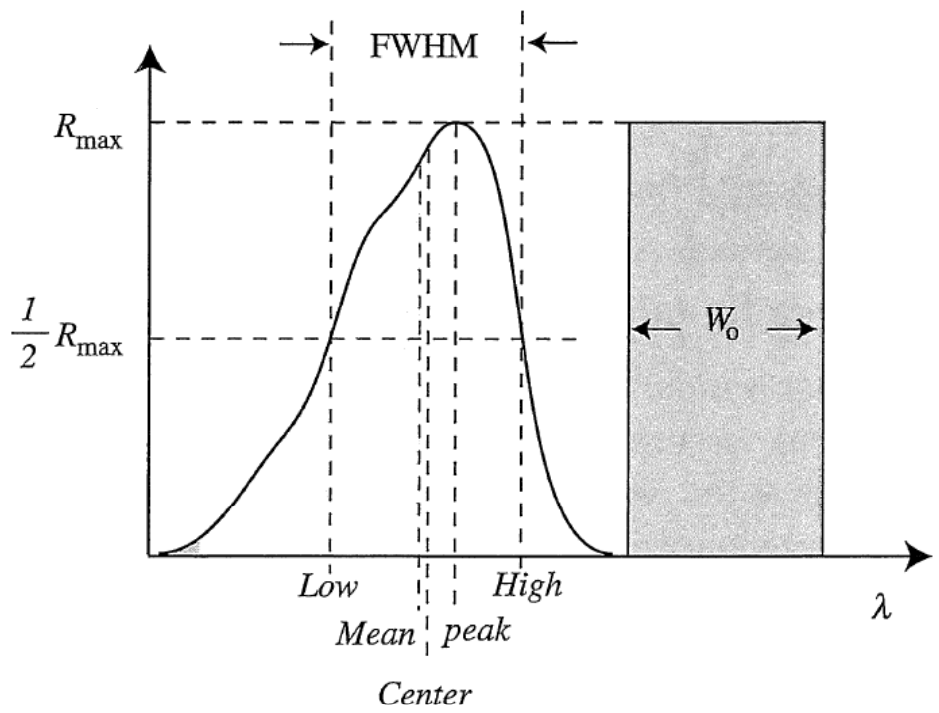

Figure 5.2. Normalized transmission curves (solid lines) for the Johnson–Cousins filters recommended by Bessell. Photon flux of Vega scaled for clarity (dotted line).

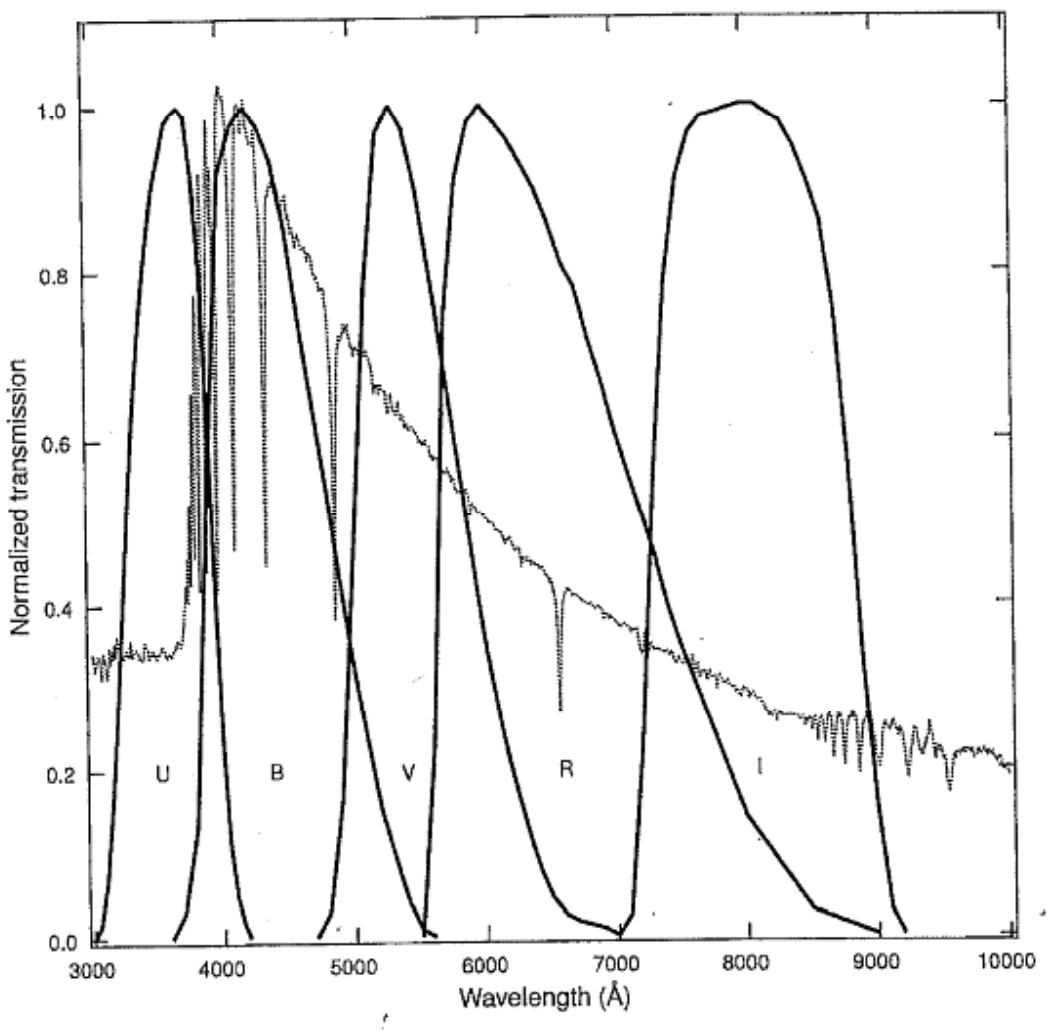

SDSS camera and filter QE

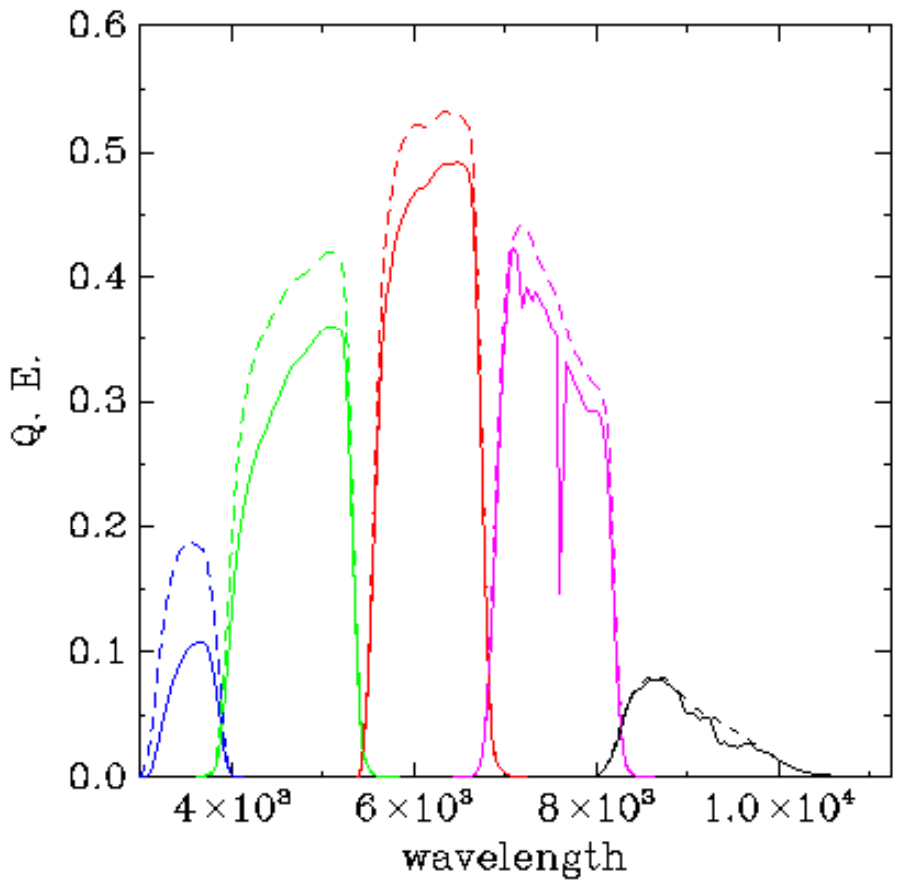

Dotted: lab
Solid: 1.3 airmasses

Near-IR bands and atmosphere for MKO and Johnson systems

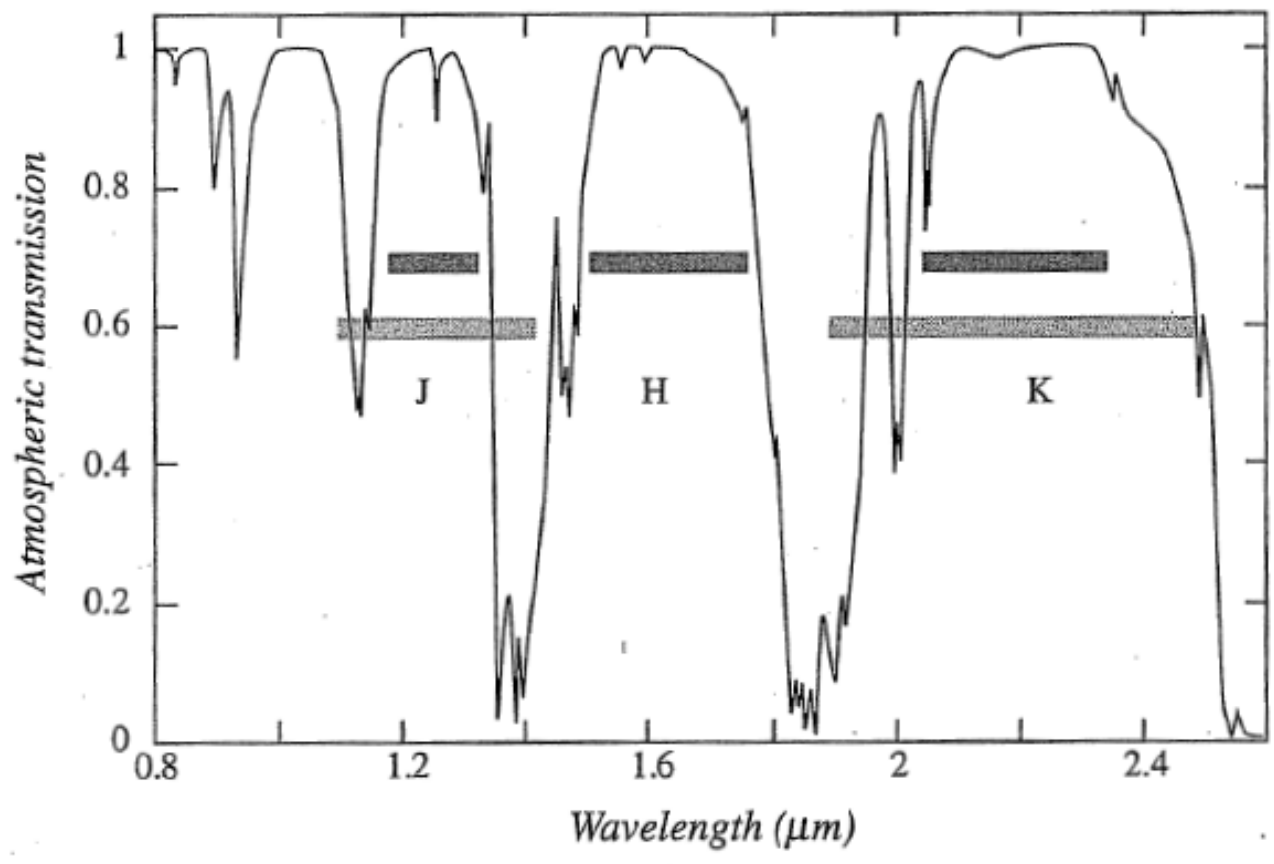

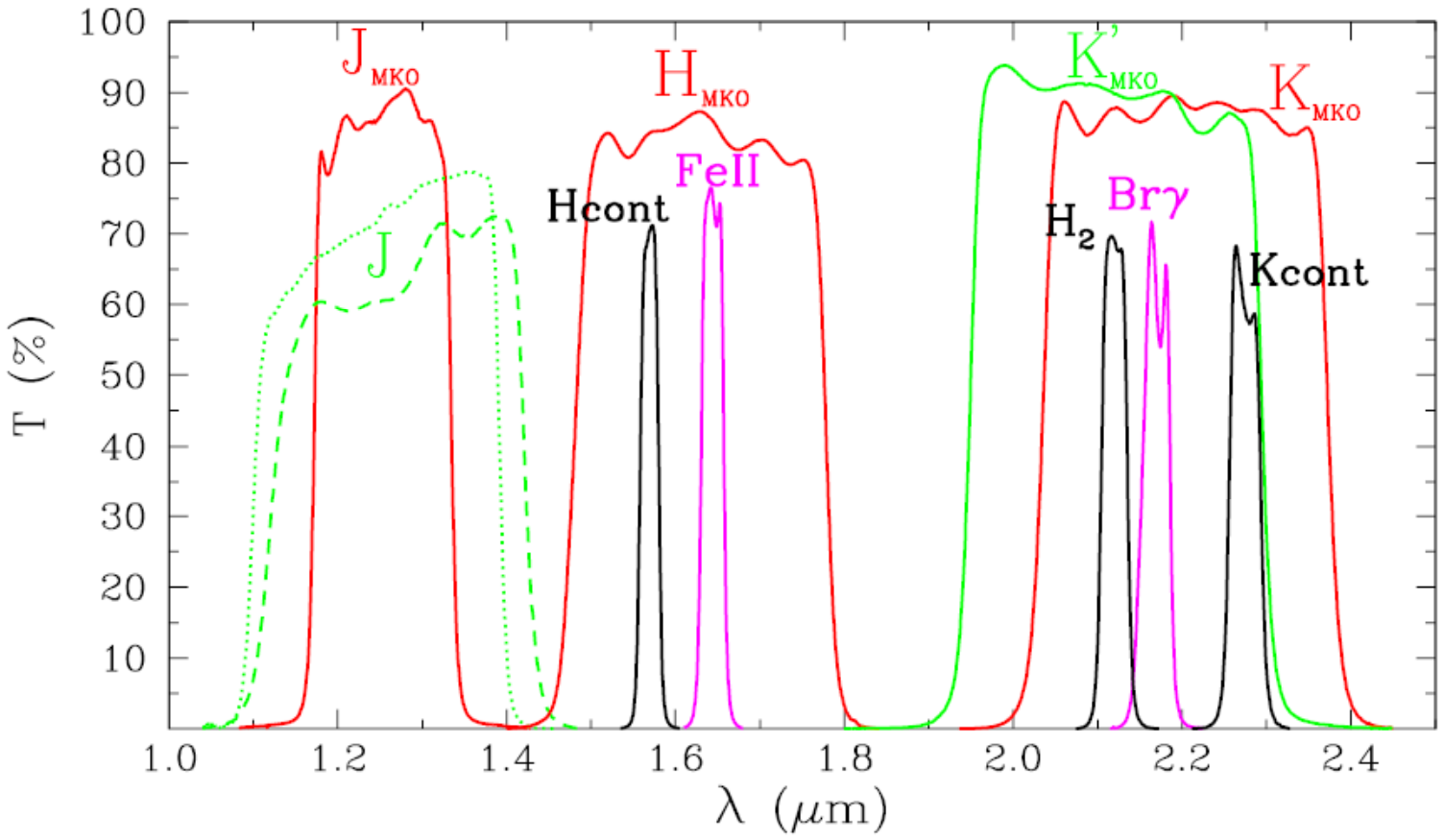

Fig. 1. Overview of the transmission curves of the filters of Mauna Kea Observatories (MKO) near infrared filter consortium. The data were taken at a temperature of 78 K and with the broad and narrow band filters illuminated at an incidence angle of 5° and 3°, respectively. For comparison, we also include the curve relative to the "standard J" filter of NICS measured in the same conditions (dashed line) as well as that of the "standard J" filter used in the SOFI and ISAAC instruments of ESO (dotted line). The data for the ESO filter were downloaded from the ISAAC web page.

Spectral discontinuities and lines

Spectral "break"

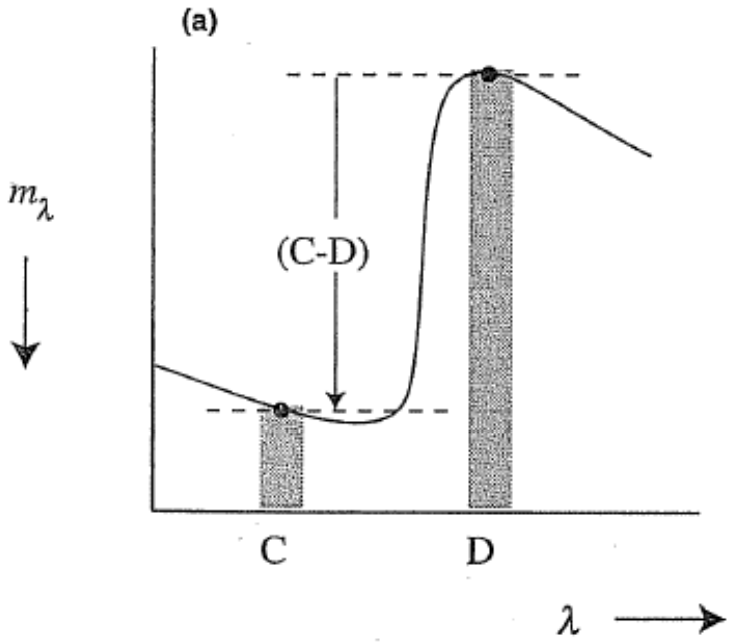

Absorption feature

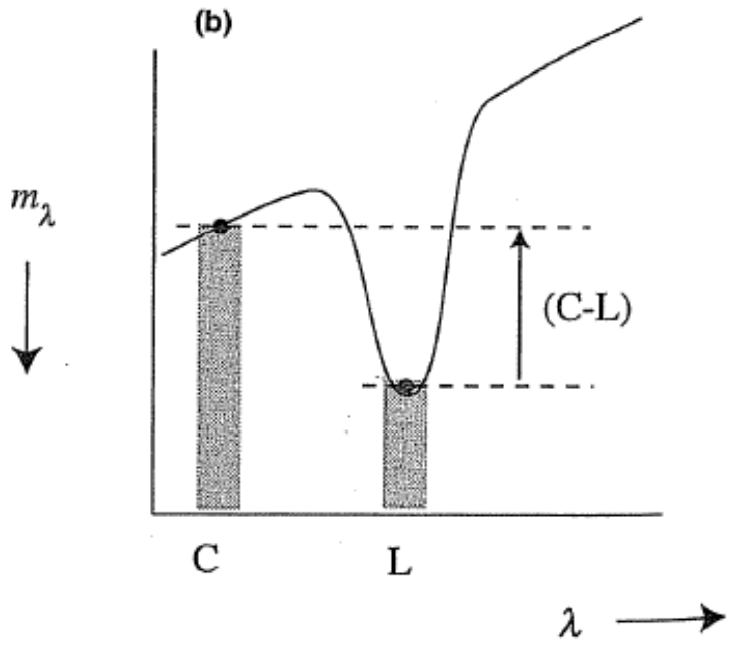

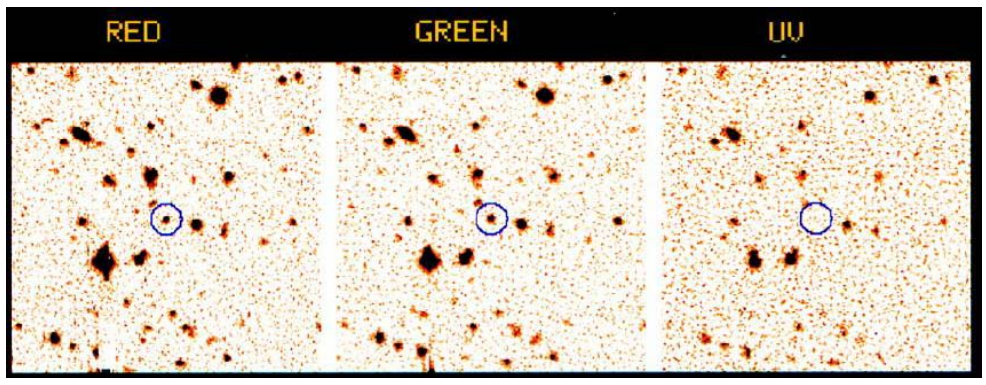

"UV dropout"

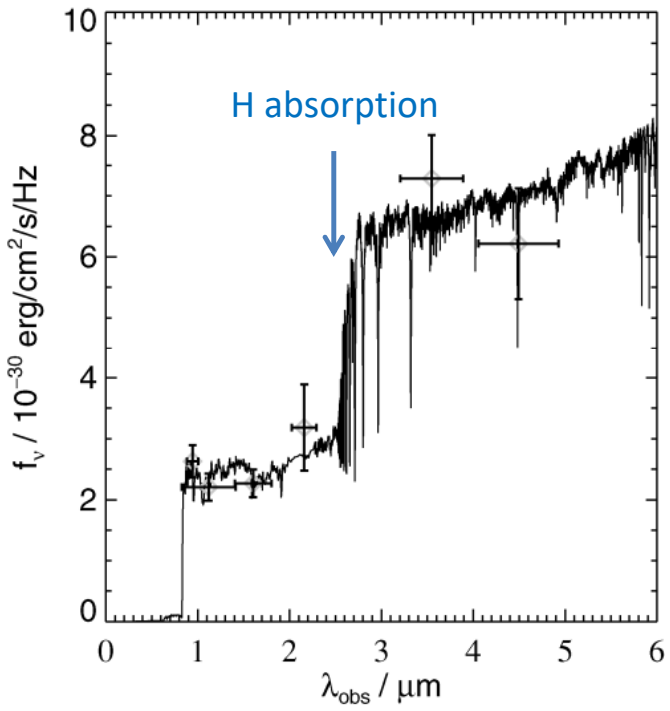

Table 5.1. *Indices of refraction. Both the index and dispersion are given at the wavelength of the Fraunhofer D line. Data after Pedrottí et. al. (2006) and the Schott Glass (2009) website**

Material	n ($\lambda = 588$ nm)	$dn/d\lambda$ (μm^{-1})	ν_D
Air (STP)	1.00029	2×10^{-5}	85
Water	1.33	0.017	114
Calcium fluoride	1.435	0.027	95
Fused quartz	1.458	0.040	68
Borosilicate crown glass (BK7)	1.517	0.047	64
Flint glass (F2)	1.620	0.100	36
Dense flint glass (SF4)	1.756	0.161	28
Diamond	2.42	0.250	33

* http://www.us.schott.com/optics_devices/english/download/kataloge.html

Fig. 5.14 Refractive index as a function of wavelength for some optical glasses in the Schott Catalog. Curves end where the glass becomes nearly opaque, except we show the curve for borosilicate crown glass (N-BK7) as a dotted line in the region where it is highly absorbing. SF4 is one of the most dispersive of the flints. N-LAK10 is an unusual crown with low dispersion and high index. SiO_2 is fused quartz, and CaF_2 is calcium fluoride.